

Electronic Supplementary Information for

Self-assembly and layer-by-layer deposition of metallosupramolecular perylene bisimide polymers

Vladimir Stepanenko,^a Michael Stocker,^b Paul Müller,^b Michael Büchner^a and Frank Würthner*^a

^a Universität Würzburg, Institut für Organische Chemie and Röntgen Research Center for Complex Material Systems, Am Hubland, 97074 Würzburg, Germany. E-mail: wuerthner@chemie.uni-wuerzburg.de

^b Universität Erlangen-Nürnberg, Department of Physics and Center for Molecular Materials (ICMM), Erwin-Rommel-Str. 1, 91058 Erlangen, Germany

Table of contents

Material and methods	2
Synthesis of perylene bisimide building blocks	3
Metal-ion-mediated self-assembly of perylene bisimide building blocks	7
Complexation of monotopic ligands with Zn(II) ion: ¹ H NMR titration experiments	9
Supramolecular polymerization of ditopic ligands by Zn(II) ion coordination: ¹ H NMR titration experiments	10
¹ H DOSY NMR investigations	11
UV-vis spectra of monotopic PBI ligands 7 and 8 , and their dimers (7)₂Zn(OTf)₂ and (8)₂Zn(OTf)₂	13
UV-vis titration spectra of ditopic PBI ligands 3 and 4a with Zn(II) triflate	14
Scanning tunneling microscope and current imaging tunneling spectroscopy measurements	15
Electrostatic self-assembly of coordination polymers: multilayer films	16
References	17

Material and methods

Solvents were purified and dried according to standard procedures.¹ Column chromatography was performed with silica gel (0.035-0.070 mm) and basic alumina, the latter was deactivated with 4 weight % of water to activity II. Zinc trifluoromethane sulfonate salt was obtained from commercial sources. MALDI-TOF mass spectra were measured using a Bruker Autoflex II spectrometer in reflector mode. ¹H NMR spectra were recorded at 298 K on a Bruker Avance 400 spectrometer (400 MHz) and chemical shifts δ (ppm) were calibrated against tetramethylsilane (Me₄Si) as internal reference. ¹H DOSY experiments were carried out at 298 K on a Bruker DMX 600 spectrometer (600 MHz) equipped with a BGPA 10 gradient generator, a BGU II control unit, and a conventional 5 mm broadband (¹⁵N-³¹P)/¹H probe with automatic tune/match accessory and z axis gradient coil capable of producing pulsed magnetic field gradients in the z direction of 52 G cm⁻¹. For the measurement of UV-vis spectra, PerkinElmer Lambda 950 spectrometer was used. The steady-state fluorescence spectra were measured on a PTI QM-4/2003 spectrometer and fluorescence quantum yields were determined by optical dilute method² ($A < 0.05$) using *N,N'*-di(2,6-diisopropylphenyl)-1,6,7,12-tetraphenoxyperylene-3,4:9,10-tetracarboxylic acid bisimide ($\Phi_{fl} = 0.96$ in chloroform)³ and Nileblue *a* ($\Phi_{fl} = 0.27$ in ethanol)⁴ as standards. The solvents for spectroscopic studies were of spectroscopic grade and used as received. Fluorescence lifetimes were determined with a fluorescence lifetime measurement system by using a PTI GL330 nitrogen laser (337 nm) and a PTI GL302 dye laser. Fluorescence decay curves were evaluated by using the software supplied with the instrument. AFM measurements were carried out under ambient conditions by using a Veeco MultiModeTM Nanoscope IV system operating in tapping mode in air.

Synthesis of perylene bisimide building blocks

N,N'-Bis(4'-2,2':6',2''-terpyridyl)-1,7-dipyrrolidinylperylene-3,4:9,10-tetracarboxylic acid bisimide (3)

A mixture of 50.0 mg (0.094 mmol) of 1,7-dipyrrolidinylperylene-3,4:9,10-tetracarboxylic acid bisanhydride⁵ (**1**) and 70.3 mg (0.28 mmol) of 4'-amino-2,2':6',2''-terpyridine⁶ was heated in pyridine/imidazole (2:1) under stirring at 120 °C for 48 h under argon. After cooling to room temperature, the mixture was poured into aqueous HCl (10 mL, 1 M). The resulting precipitate was separated by filtration, washed with water (6 × 50 mL) and purified by column chromatography with dichloromethane/acetone (97:3) to yield 55 mg (59%) of **3** as a dark-green powder.

Mp > 350 °C; *m/z* (FAB) = 991.59 [M⁺], 992.60 [M⁺+H] calc. for C₆₂H₄₂N₁₀O₄ 991.06; *m/z* (HRMS, ESI, pos.) = 990.3385 [M⁺] calc. for C₆₂H₄₂N₁₀O₄ 990.3390; δ_H (400 MHz, CDCl₃, Me₄Si): 8.71 (d, *J* = 6.9 Hz, 4H, H_{6,6''}), 8.68 (d, *J* = 5.6 Hz, 4H, H_{3,3''}), 8.57 (s, 2H, H_{per}), 8.55 (s, 4H, H_{3',5'}), 8.53 (d, *J* = 8.0 Hz, 2H, H_{per}), 7.87-7.91 (m, 4H, H_{4,4''}), 7.80 (d, *J* = 8.0 Hz, 2H, H_{per}), 7.32-7.35 (m, 4H, H_{5,5''}), 3.72-3.91 (m, 4H, H_{Pyrrolidinyl}), 2.87-3.02 (m, 4H, H_{Pyrrolidinyl}), 1.97-2.18 (m, 8H, H_{Pyrrolidinyl}); λ_{max}(CH₂Cl₂)/nm = 714 (ε/M⁻¹cm⁻¹ 48200), 437 (18900), 279 (67000), 250 (89200); fluorescence λ_{max} (CH₂Cl₂, λ_{ex} = 660 nm)/nm = 750, quantum yield Φ_f (CH₂Cl₂) = 0.26±0.01; fluorescence lifetime τ (CH₂Cl₂, λ_{ex} = 660 nm, λ_{em} = 745 nm)/ns = 3.8±0.2.

N,N'-Bis(4'-2,2':6',2''-terpyridyl)-1,6,7,12-tetra(4-*t*-octylphenoxy)perylene-3,4:9,10-tetracarboxylic acid bisimide (4a)

1,6,7,12-Tetra(4-*tert*-octylphenoxy)perylene-3,4:9,10-tetracarboxylic acid bisanhydride⁷ (**2a**) (0.13 mg, 0.11 mmol) was reacted with 4'-amino-2,2':6',2''-terpyridine (0.79 g, 0.32 mmol) in pyridine/imidazole (2:1) for 24 h at 120 °C under argon. After cooling to room temperature, the mixture was poured into aqueous HCl (70 mL, 1 M); the resulting precipitate was isolated by filtration and subsequently washed

with water (20 mL) and methanol (20 mL). Purification was achieved by column chromatography on aluminium oxide (basic, activity II) with CH₂Cl₂/n-hexane (80:20) to yield **4a** (83 mg, 46%) as a dark-red microcrystalline powder.

Mp > 350 °C; *m/z* (FAB) = 1670.3 [M⁺], 1671.3 [M⁺+H], calc. for C₁₁₀H₁₀₈N₈O₈ 1670.08; δ_H (400 MHz, CDCl₃, Me₄Si): 8.65 (d, *J* = 6.9 Hz, 4H, H6,6''), 8.64 (d, *J* = 4.8 Hz, 4H, H3,3''), 8.45 (s, 4H, H3',5'), 8.21 (s, 4H, H_{per}y), 7.81-7.86 (m, 4H, H4,4''), 7.25-7.31 (m, 12H, H_{Ar}, H5,5''), 6.91 (d, *J* = 8.7 Hz, 8H, H_{Ar}), 1.70-2.18 (s, 12H, CH₂), 1.33 (s, 24H, CH₃), 0.74 (s, 36H, CH₃); λ_{max} (CH₂Cl₂)/nm = 588 (ε/M⁻¹cm⁻¹ 50800), 550 (30300), 456 (17200), 283 (82200), 239 (106800); fluorescence λ_{max} (CH₂Cl₂, λ_{ex} = 540 nm)/nm = 618, quantum yield Φ_{fl}(CH₂Cl₂) = 0.96±0.01; fluorescence lifetime τ (CH₂Cl₂, λ_{ex} = 540 nm, λ_{em} = 617 nm)/ns = 6.6±0.2; found: C 78.73, H 6.81, N 6.55; calc. for C₁₁₀H₁₀₈N₈O₈ (1670.3): C 79.11, H 6.52, N 6.71.

N,N'-Bis(4'-2,2':6',2''-terpyridyl)-1,6,7,12-tetra(4-*tert*-butylphenoxy)perylene-3,4:9,10-tetracarboxylic acid bisimide (4b**)**

This compound was synthesized and purified according to procedure as described for **4a** from 1,6,7,12-tetra(4-*tert*-butylphenoxy)perylene-3,4:9,10-tetracarboxylic acid bisanhydride⁷ (**2b**) (0.15 g, 0.15 mmol) and 4'-amino-2,2':6',2''-terpyridine (0.15 g, 0.61 mmol), to give **4b** (0.11 g, 50%) as a bright-red powder.

Mp > 350 °C; *m/z* (FAB) = 1445.5 [M⁺], calc. for C₉₄H₇₆N₈O₈ 1445.6; *m/z* (HRMS, ESI, pos.) = 1445.5859 [M⁺], calc. for C₉₄H₇₆N₈O₈ 1445.5820; δ_H (400 MHz, CDCl₃, Me₄Si): 8.65 (d, *J* = 6.9 Hz, 4H, H6,6''), 8.64 (d, *J* = 4.8 Hz, 4H, H3,3''), 8.46 (s, 4H, H3',5'), 8.28 (s, 4H, H_{per}y), 7.82-7.88 (m, 4H, H4,4''), 7.29-7.33 (m, 4H, H5,5''), 7.24 (d, 8H, *J* = 8.7 Hz, H_{Ar}), 6.88 (d, *J* = 8.7 Hz, 8H, H_{Ar}), 1.26 (s, 36H, CH₃); λ_{max} (CH₂Cl₂)/nm = 585 (ε/M⁻¹cm⁻¹ 54200), 544 (32500), 454 (18400), 281 (89400); fluorescence λ_{max} (CH₂Cl₂, λ_{ex} = 540 nm)/nm = 615, quantum yield Φ_{fl}(CH₂Cl₂) = 0.97±0.01.

N-Cyclohexyl-N'-(4'-2,2':6',2''-terpyridyl)-1,7-dipyrrolidinylperylene-3,4:9,10-tetracarboxylic

acid bisimide (7)

N-Cyclohexyl-1,7-dipyrrolidinylperylene-3,4:9,10-tetracarboxylic acid-3,4-anhydride-9,10-imide⁵ (**5**) (150 mg, 0.25 mmol) was reacted with 4'-amino-2,2':6',2''-terpyridine (91.3 g, 0.37 mmol) in pyridine/imidazole (2:1) for 50 h at 120 °C under argon. After cooling to room temperature, the mixture was poured into aqueous HCl (20 mL, 1 M); the resulting precipitate was extracted with 90 mL of methylene chloride, washed with water, dried over MgSO₄, and concentrated by rotary evaporation. Purification was achieved by column chromatography on silica gel with CH₂Cl₂/methanol (99:1) to yield **7** (140 mg, 68%) as a dark-green microcrystalline powder.

Mp > 330 °C; *m/z* (MALDI-TOF, dithranol) = 841.18 [M⁺], 842.18 [M⁺+H] calc. for C₅₃H₄₃N₇O₄ 841.95; δ_H (400 MHz, CDCl₃, Me₄Si): 8.70 (d, *J* = 7.9 Hz, 2H, H_{6,6''}), 8.67 (d, *J* = 4.4 Hz, 2H, H_{3,3''}), 8.54 (s, 1H, H_{pery}), 8.54 (s, 2H, H_{3',5'}), 8.51 (s, 1H, H_{pery}), 8.49 (d, *J* = 9.4 Hz, 1H, H_{pery}), 8.44 (d, *J* = 8.1 Hz, 1H, H_{pery}), 7.85-7.89 (m, 2H, H_{4,4''}), 7.80 (d, *J* = 8.0 Hz, 1H, H_{pery}), 7.75 (d, *J* = 8.0 Hz, 1H, H_{pery}), 7.32-7.35 (m, 2H, H_{5,5''}), 5.00-5.14 (m, 1H, NCH₂), 3.70-3.90 (m, 4H, H_{Pyrrolidinyl}), 2.80-3.00 (m, 4H, H_{Pyrrolidinyl}), 2.56-2.67 (m, 2H, H_{Cy}), 1.89-2.10 (m, 10H, H_{Pyrrolidinyl}, H_{Cy}), 1.72-1.80 (m, 2H, H_{Cy}), 1.33-1.50 (m, 4H, H_{Cy}); δ_C (100 MHz, CDCl₃): 164.6, 164.5, 163.6, 163.5, 157.1, 155.7, 149.1, 146.8, 146.4, 145.9, 136.8, 135.1, 134.0, 130.3, 130.0, 127.3, 126.6, 124.2, 123.9, 123.8, 122.8, 122.7, 122.3, 121.6, 121.4, 121.3, 121.2, 120.8, 119.9, 118.9, 118.7, 117.7 53.8, 52.3, 29.2, 26.7, 25.8, 25.6; λ_{max}(CH₂Cl₂)/nm = 706 (ε/M⁻¹cm⁻¹ 41800), 436 (16600), 309 (35600), 278 (44300), 246 (69500); fluorescence λ_{max}(CH₂Cl₂, λ_{ex} = 660 nm)/nm = 746, quantum yield Φ_{fl}(CH₂Cl₂) = 0.19; fluorescence lifetime τ(CH₂Cl₂, λ_{ex} = 660 nm, λ_{em} = 745 nm)/ns = 3.7±0.2; found: C 73.86, H 5.36, N 11.42; calc. for C₅₃H₄₃N₇O₄×H₂O (859.9): C 73.95, H 5.01, N 11.30.

N-Butyl-N'-(4'-2,2':6',2''-terpyridyl)-1,6,7,12-tetra(4-*tert*-butylphenoxy)perylene-3,4:9,10-tetracarboxylic acid bisimide (8)

N-Butyl-1,6,7,12-tetra(4-*tert*-butylphenoxy)perylene-3,4:9,10-tetracarboxylic acid-3,4-anhydride-9,10-imide⁷ (**6**) (0.14 mg, 0.13 mmol) was reacted with 4'-amino-2,2':6',2''-terpyridine (0.50 g, 0.20 mmol) in pyridine/imidazole (2:1) for 48 h at 120 °C under argon. After cooling to room temperature, the mixture was poured into aqueous HCl (20 mL, 1 M); the resulting precipitate was isolated by filtration and subsequently washed with water (30 mL) and methanol (20 mL). Purification was achieved by column chromatography on aluminium oxide (basic, activity II) with CH₂Cl₂/*n*-hexane (80:20) to yield **6** (84 mg, 50%) as a dark-red microcrystalline powder.

Mp > 320 °C; *m/z* (ESI, pos.) = 1270.56 [M⁺], calc. for C₈₃H₇₅N₅O₈ 1270.55; δ_H (400 MHz, CDCl₃, Me₄Si): 8.58 (m, 4H, H_{6,6'',H3,3''}), 8.39 (s, 1H, H_{3',5'}), 8.18 (s, 2H, H_{pery}), 8.17 (s, 2H, H_{pery}), 7.79 (m, 2H, H_{4,4''}), 7.25 (m, 2H, H_{5,5''}), 7.17 (m, 8H, H_{Ar}), 6.78 (m, 8H, H_{Ar}), 4.05 (m, 2H, NCH₂), 1.61 (m, 2H, CH₂), 1.34 (m, 2H, CH₂), 1.22 (s, 18H, CH₃), 1.18 (s, 18H, CH₃); λ_{max} (CH₂Cl₂)/nm = 581 (ε/M⁻¹cm⁻¹ 46100), 541 (27800), 453 (16600), 285 (64000); fluorescence λ_{max} (CH₂Cl₂, λ_{max} = 540 nm)/nm = 611, quantum yield Φ_f(CH₂Cl₂) = 0.89±0.01; fluorescence lifetime τ (CH₂Cl₂, λ_{ex} = 540 nm, λ_{em} = 617 nm)/ns = 7.2±0.2; found: C 78.18, H 5.86, N 5.42; calc. for C₈₃H₇₅N₅O₈ (1270.56): C 78.46, H 5.95, N 5.51.

Metal-ion-mediated self-assembly of perylene bisimide building blocks

Metallocidimer (7**)₂Zn(OTf)₂**

To a solution of *N*-cyclohexyl-*N'*-(4'-2,2':6',2"-terpyridyl)-1,7-dipyrrolidinylperylene-3,4:9,10-tetracarboxylic acid bisimide **7** (10.0 mg, 11.8 μ mol) in CHCl₃/CH₃OH (60:40, 0.65 mL) a stock solution of zinc triflate (16.8 mM, 350 μ L, 5.9 μ mol) was added and the solution was stirred for 10 min at room temperature. The solution was concentrated by rotary evaporation; the product was precipitated by addition of acetonitrile (10 mL) and isolated quantitatively by centrifugation. Exact 2:1 stoichiometry of **7** and zinc triflate was confirmed by ¹H NMR.

m/z (MALDI-TOF, dithranol) = 1895.50 [M-OTf]⁺, 1746.50 [M-2OTf]⁺, 1054.20 [7+Zn+OTf]⁺ calc. for C₁₀₈H₈₆F₆N₁₄O₁₄S₂Zn 2045.51; δ _H (400 MHz, CDCl₃/CD₃OD 60:40, Me₄Si): 9.11 (bs, 4H, H_{3',5'}), 8.76 (d, *J* = 8.1 Hz, 4H, H_{3,3''}), 8.58 (bs, 4H, H_{per}), 8.42-8.49 (m, 4H, H_{per}), 8.25-8.35 (m, 4H, H_{4,4''}), 8.07 (d, *J* = 4.7 Hz, 4H, H_{6,6''}), 7.75-7.85 (m, 2H, H_{per}), 7.61-7.67 (m, 4H, H_{5,5''}), 7.53-7.61 (m, 2H, H_{per}), 5.08-5.15 (m, 2H, NCH₂), 3.68-3.87 (m, 8H, H_{Pyrrolidinyl}), 2.73-2.92 (m, 8H, H_{Pyrrolidinyl}), 2.61-2.72 (m, 4H, H_{Cy}), 1.77-2.16 (m, 28H, H_{Pyrrolidinyl}, H_{Cy}), 1.38-1.56 (m, 4H, H_{Cy}); λ_{max} (CHCl₃/MeOH 60:40)/nm = 723 (ϵ /M⁻¹cm⁻¹ 78400), 441 (32000), 320 (66800), 285 (90200); fluorescence λ_{max} (DMF, $\lambda_{\text{ex}} = 660$ nm)/nm = 764, quantum yield Φ_{fl} (DMF) = 0.10±0.01; fluorescence lifetime τ (CHCl₃/MeOH 60:40), $\lambda_{\text{ex}} = 660$ nm, $\lambda_{\text{em}} = 770$ nm)/ns = 1.8±0.2.

Metallocidimer (8**)₂Zn(OTf)₂**

To a solution of *N*-butyl-*N'*-(4'-2,2':6',2"-terpyridyl)-1,6,7,12-tetra(4-*t*-butylphenoxy)perylene-3,4:9,10-tetracarboxylic acid bisimide **8** (4.94 mg, 3.88 μ mol) in CHCl₃/CH₃OH (60:40, 0.70 mL) a stock solution of zinc triflate (4.85 mM, 400 μ L, 1.94 μ mol) was added and the solution was stirred for 10 min at room temperature. The solution was concentrated by rotary evaporation; the product was precipitated by addition of acetonitrile (10 mL) and isolated quantitatively by centrifugation. Exact 2:1

stoichiometry of ligand **8** and Zn(II) triflate was confirmed by ^1H NMR.

m/z (MALDI-TOF, DCTB) = 2754.0 [M-OTf] $^+$, 2605.0 [M-2OTf] $^+$ calc. for C₁₆₈H₁₅₀F₆N₁₀O₂₂S₂Zn 2904.5; δ_{H} (400 MHz, CDCl₃/CD₃OD 60:40, Me₄Si): 8.92 (s, 4H, H_{3',5'}), 8.59 (d, J = 8.1 Hz, 4H, H_{3,3''}), 8.37 (s, 4H, H_{pery}), 8.26 (s, 4H, H_{pery}), 8.16-8.22 (m, 4H, H_{4,4''}), 7.87 (d, J = 5.6 Hz, 4H, H_{6,6''}), 7.47-7.54 (m, 4H, H_{5,5''}), 7.27-7.33 (m, 16H, H_{Ar}), 6.90-6.95 (m, 16H, H_{Ar}), 4.11-4.17 (m, 4H, NCH₂), 1.66-1.72 (m, 4H, CH₂), 1.38-1.46 (m, 4H, CH₂), 1.32 (s, 36H, CH₃), 1.29 (s, 36H, CH₃), 0.93-0.99 (m, 6H, CH₃); λ_{max} (CHCl₃/MeOH 60:40)/nm = 591 ($\epsilon/\text{M}^{-1}\text{cm}^{-1}$ 100700), 552 (61200), 458 (36100), 332 (30600), 285 (136000), 267 (133100); fluorescence λ_{max} (CHCl₃/MeOH 60:40, $\lambda_{\text{ex}} = 540$ nm)/nm = 625 nm, quantum yield Φ_{fl} (CHCl₃/MeOH 60:40) = 0.82±0.02; fluorescence lifetime τ (CHCl₃/MeOH 60:40), $\lambda_{\text{ex}} = 540$ nm, $\lambda_{\text{em}} = 617$ nm)/ns = 7.6±0.2.

Complexation of monotopic ligands with Zn(II) ion: ^1H NMR titration experiments

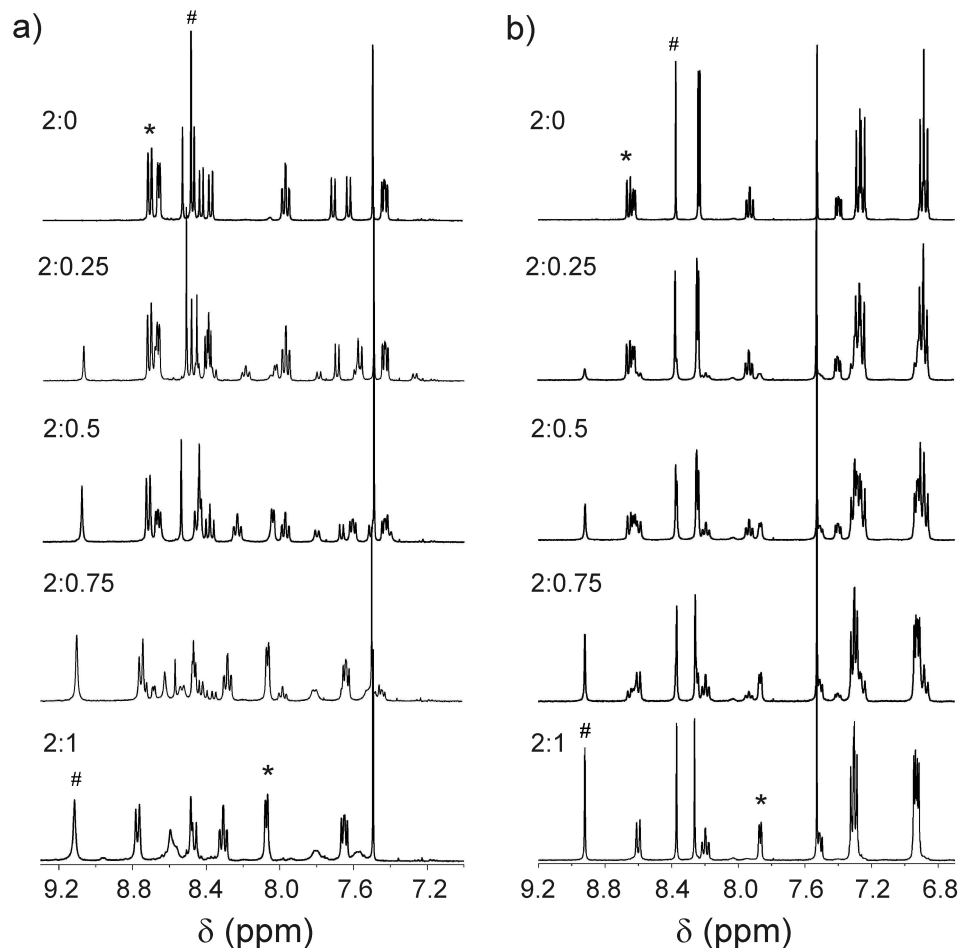


Fig. S1 Aromatic regions of ^1H NMR spectra recorded at different ligand/Zn(II) ion ratios (2:0 to 2:1) at 298 K: a) For the monotopic ligand **7** and zinc triflate in $\text{CDCl}_3/\text{CD}_3\text{OD}$ (60:40, 5 mM) from free ligand **7** (upper spectrum) to dimer $(\text{7})_2\text{Zn}(\text{OTf})_2$ (bottom); b) for the monotopic ligand **8** and zinc triflate in $\text{CDCl}_3/\text{CD}_3\text{OD}$ (60:40, 3.5 mM) from free ligand **8** (upper spectrum) to dimer $(\text{8})_2\text{Zn}(\text{OTf})_2$ (bottom). The ratio of **7**:Zn(II) ion (a) or **8**:Zn(II) ion (b) is indicated on the respective spectrum. Signals for $\text{H}3',5'$ protons are marked with # and those of $\text{H}6,6''$ protons with *.

Supramolecular polymerization of ditopic ligand **4a by Zn(II) ion coordination: ^1H NMR titration experiments**

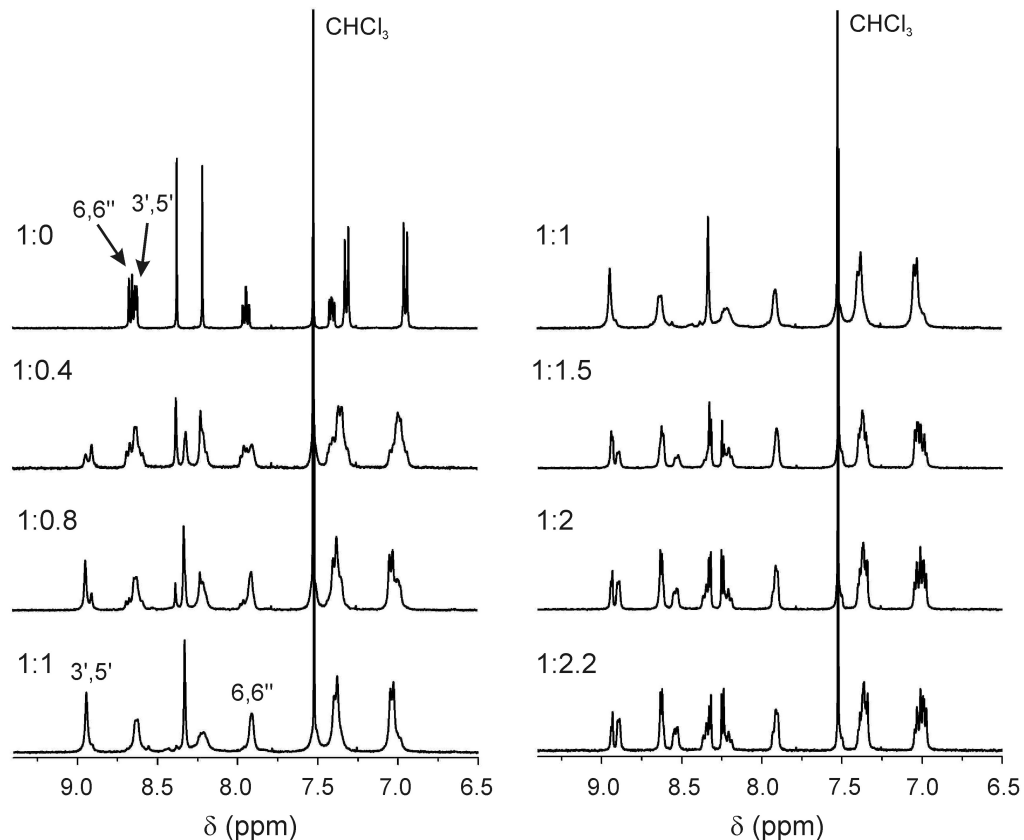


Fig. S2 Aromatic regions of ^1H NMR spectra recorded at different ligand/Zn(II) ion ratios for the bis(tpy)-PBI ligand **4a** and zinc triflate in $\text{CDCl}_3/\text{CD}_3\text{OD}$ (60:40, 3.5 mM) at 298 K from free ligand **4a** (upper spectrum, left) to polymer **10** (bottom, left) and the fragmented form **12** (bottom, right). The ratio of ligand **4a**/Zn(II) ion is indicated on the respective spectrum.

¹H DOSY NMR investigations

To provide further evidence for the formation of coordination polymers by Zn(II)-ion-mediated self-assembly of ditopic ligands **3** and **4a**, ¹H NMR diffusion-ordered spectroscopy (DOSY)⁸ experiments were performed. DOSY NMR spectroscopy has recently been successfully applied to characterize supramolecular coordination polymers, whose labile and dynamic nature quite often limits the success of conventional techniques for their characterization.⁹ The DOSY spectra were measured in chloroform-d/methanol-d₄ (60:40) mixture at 298 K first only for the ditopic ligands **3** and **4a** without Zn(OTf)₂, and then after addition of one equivalent of Zn(OTf)₂ to the solution of the respective ligand and subsequently after the addition of 2 equivalents of zinc(II) triflate. The ¹H DOSY NMR spectra for ditopic ligands **3** and **4a** are shown in Fig. S3a and S3d. The ditopic ligand **3** with a molecular weight of 991.6 g/mol shows a diffusion coefficient of $D = 3.76 \times 10^{-10} \text{ m}^2\text{s}^{-1}$ ($\log(D/\text{m}^2\text{s}^{-1}) = -9.42$) and the bis(tpy)-PBI ligand **4a** with a higher molecular weight of 1670.3 g/mol exhibits a little smaller diffusion coefficient of $D = 3.47 \times 10^{-10} \text{ m}^2\text{s}^{-1}$ ($\log(D/\text{m}^2\text{s}^{-1}) = -9.46$). A significant decrease of the D values to $D = 7.19 \times 10^{-11} \text{ m}^2\text{s}^{-1}$ ($\log(D/\text{m}^2\text{s}^{-1}) = -10.14$) and $5.84 \times 10^{-11} \text{ m}^2\text{s}^{-1}$ ($\log(D/\text{m}^2\text{s}^{-1}) = -10.23$), respectively, was observed when one equivalent of Zn(OTf)₂ was added to **3** or **4a** (see Fig. S3b and S3e). These diffusion coefficient values are one order of magnitude smaller than those of the respective ditopic monomers, indicating formation of coordination polymers upon addition of 1 equivalent of Zn(OTf)₂. When an excess amount of Zn(II) ion was added, a strong increase of the diffusion coefficients was observed, pointing at the fragmentation of the coordination polymers to oligomeric species with smaller molecular weight (Fig. S3c and S3f). At a 1:2 stoichiometry of ligand/zinc(II) ion, the diffusion coefficients are increased to $D = 2.22 \times 10^{-10} \text{ m}^2\text{s}^{-1}$ ($\log(D/\text{m}^2\text{s}^{-1}) = -9.65$) and $2.45 \times 10^{-10} \text{ m}^2\text{s}^{-1}$ ($\log(D/\text{m}^2\text{s}^{-1}) = -9.61$), which are pretty close to the values for monomeric ligands **3** and **4a**,

respectively, suggesting fragmentation of polymers into monomeric complexes **11** and **12**.

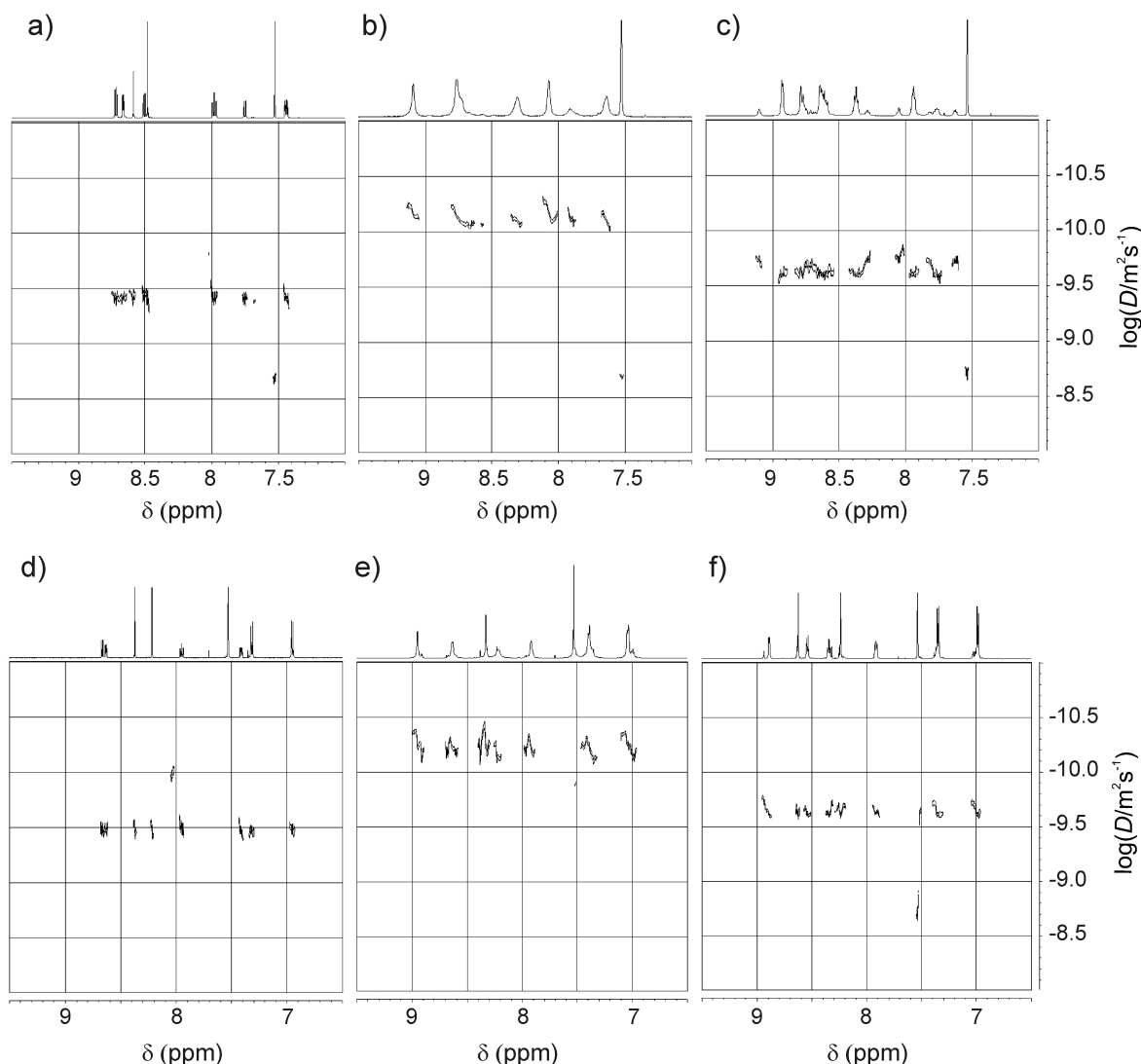


Fig. S3 Aromatic regions of the ^1H DOSY NMR spectra for bis(tpy)-PBI ligands **3** (a) and **4a** (d), supramolecular polymers **9** (b) and **10** (e), and complexes **11** (c) and **12** (f) in chloroform-d/methanol-d₄ (60:40) at 298 K; $[3] = 4.9 \times 10^{-3}$ M, $[4a] = 3.6 \times 10^{-3}$ M. The diffusion coefficients D (m^2s^{-1}) are plotted in a logarithmic scale ($\log(D/\text{m}^2\text{s}^{-1})$) against the chemical shift δ . The signal of residual chloroform can be seen at 7.51 ppm ($\log(D/\text{m}^2\text{s}^{-1}) = -8.65$).

UV-vis spectra of monotopic PBI ligands **7 and **8**, and their dimers $(\text{7})_2\text{Zn}(\text{OTf})_2$ and $(\text{8})_2\text{Zn}(\text{OTf})_2$**

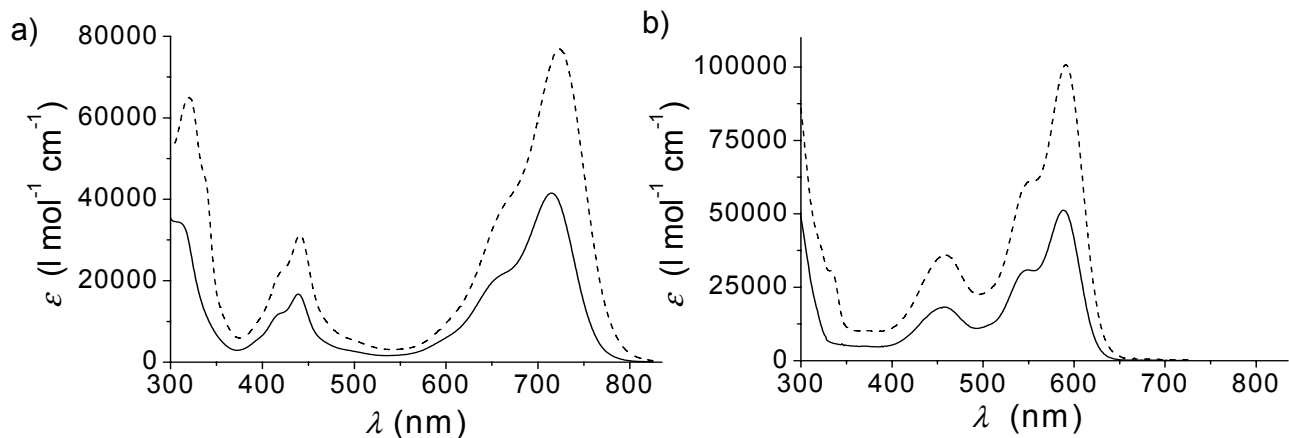


Fig. S4 UV-vis absorption spectra of a) monotopic PBI ligand **7** (solid line) and dimer $(\text{7})_2\text{Zn}(\text{OTf})_2$ (dashed line), and b) monotopic PBI ligand **8** (solid line) and dimer $(\text{8})_2\text{Zn}(\text{OTf})_2$ (dashed line) in $\text{CHCl}_3/\text{MeOH}$ (60:40) at 25 °C.

UV-vis titration spectra of ditopic PBI ligands **3 and **4a** with Zn(II) triflate**

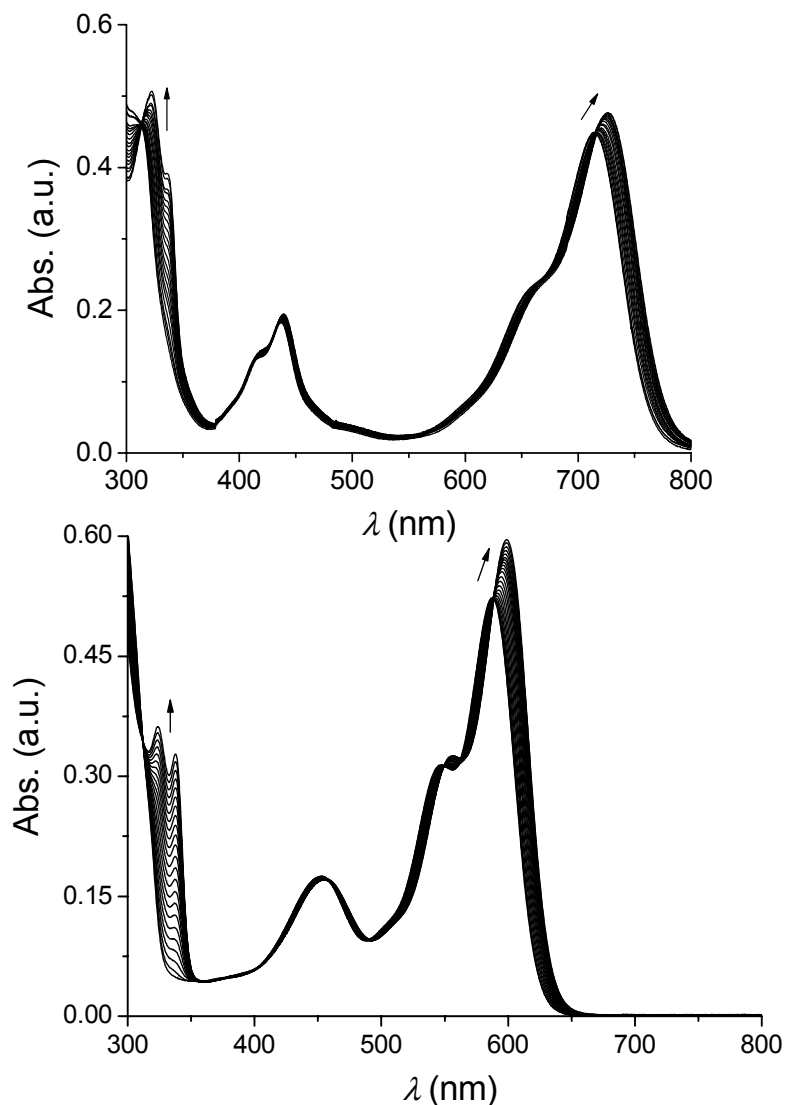


Fig. S5 UV-vis titration spectra of ditopic PBI ligand **3** (upper) and **4a** (bottom) ($c = 1 \times 10^{-5}$ M) with zinc(II) triflate in $\text{CHCl}_3/\text{CH}_3\text{CN}$ (60:40) at 25 °C. The arrows indicate the spectral changes with increasing amounts of Zn(II) ions.

Scanning tunneling microscopy and current imaging tunneling spectroscopy measurements

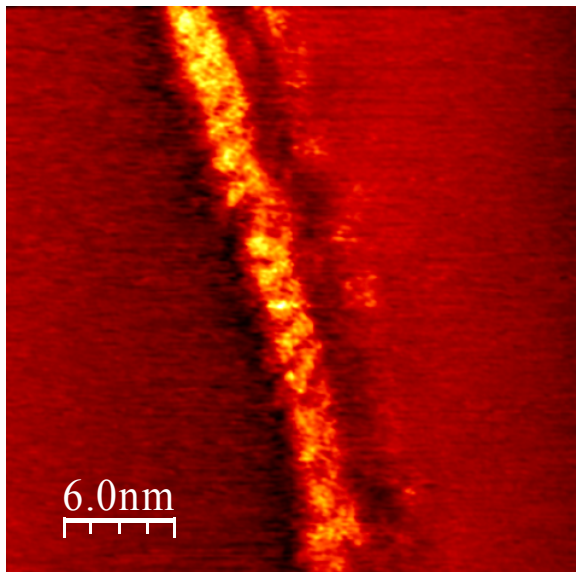


Fig. S6 30 nm × 30 nm STM scan of polymer **10** attached to a HOPG defect. Bias voltage: 100 mV; tunneling current setpoint: 30 pA. Width of the chain varies between 1.9-2.5 nm. The internal structure was not explored.

Electrostatic self-assembly of coordination polymers: layer-by-layer multifilm

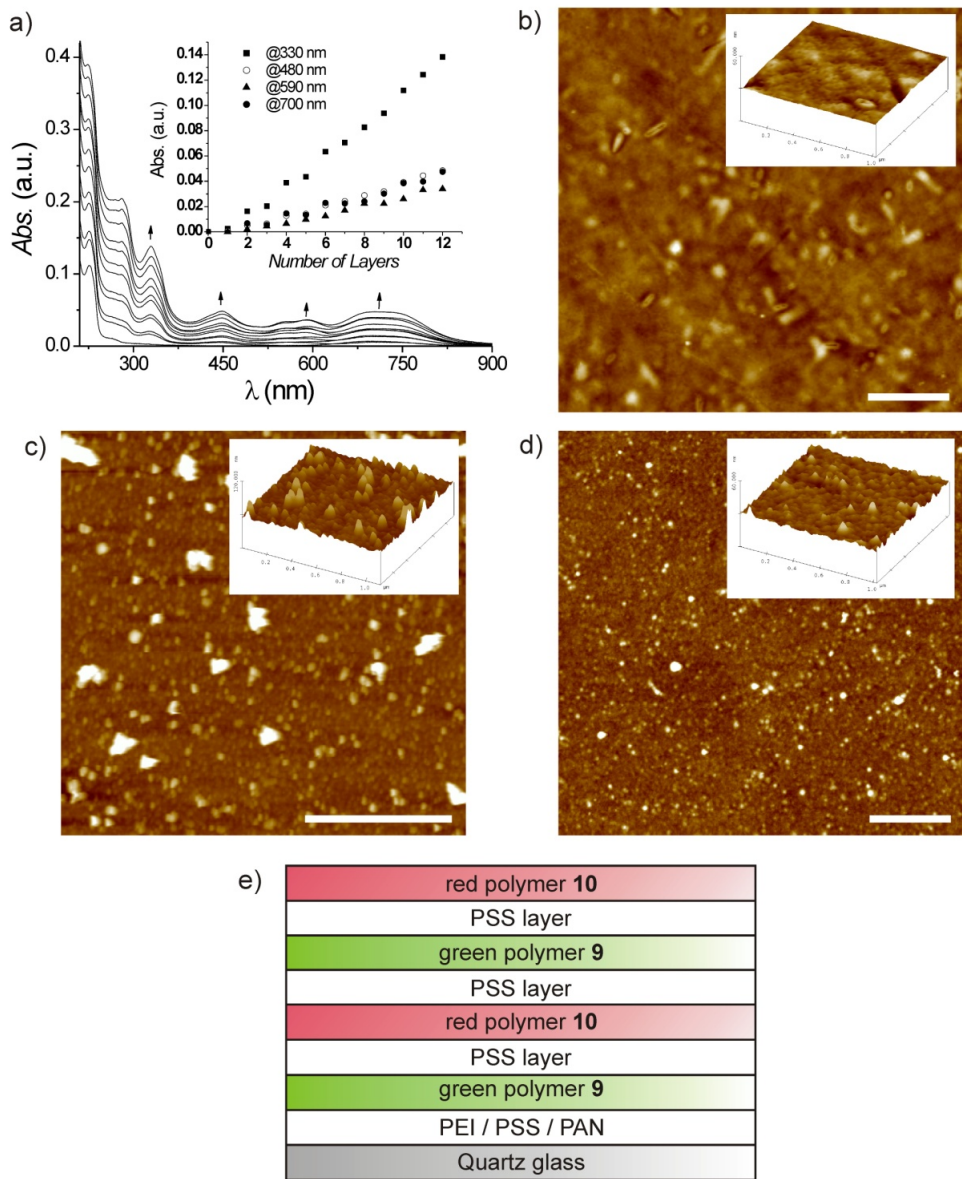


Fig. S7 (a) UV-vis spectra of self-assembled alternate multilayers [Quartz/PEI/(PSS/**9**)₆/(PSS/**10**)₆]. The inset shows the absorbance at the absorption peaks 330 (■), 480 (○), 590 (▲), and 700 nm (●) as a function of the number of layers of coordination polymers **9** and **10**. The arrows indicate the change of absorbance with increasing number of layers. (b-d) Height AFM images of quartz substrate (b), PEI/PSS

layer (c), and film after deposition of coordination polymers (d); the white scale bar in all images is 1 μm ; z data scales are 15 (b), 70 (c), and 25 nm (d). The insets in (b-d) depict AFM angle view images. (e) Schematic representation of layer-by-layer film prepared in alternate fashion.

References

1. D. D. Perrin and W. L. F. Armarego, *Purification of Laboratory Chemicals*; Pergamon Press, Oxford, 1980, 2nd edn.
2. J. R. Lakowicz, *Principles of Fluorescence Spectroscopy*; Kluwer Academic Plenum, New York, 1999, 2nd edn.
3. (a) G. Seybold and G. Wagenblast, *Dyes Pigm.*, 1989, **11**, 303; (b) R. Gvishi, R. Reisfeld and Z. Burshtein, *Chem. Phys. Lett.*, 1993, **213**, 338.
4. R. Sens and K. H. Drexhage, *J. Luminesc.*, 1981, **24**, 709.
5. F. Würthner, V. Stepanenko, Z. Chen, C. R. Saha-Möller, N. Kocher and D. Stalke, *J. Org. Chem.*, 2004, **69**, 7933.
6. R.-A. Fallahpour, M. Neuburger and M. Zehnder, *New J. Chem.*, 1999, **23**, 53.
7. (a) F. Würthner, C. Thalacker, A. Sautter, W. Schärtl, W. Ibach and O. Hollricher, *Chem. Eur. J.*, 2000, **6**, 3871; (b) D. Dotcheva, M. Klapper and K. Müllen, *Macromol. Chem. Phys.*, 1994, **195**, 1905; (c) M. Thelakkat, P. Posch and H.-W. Schmidt, *Macromolecules*, 2001, **34**, 7441.
8. (a) T. W. Claridge, *High-Resolution NMR Techniques in Organic Chemistry*; T.O.C. Series, Pergamon-Press, Amsterdam, 1999; (b) C. S. Johnson, Jr., *Prog. Nucl. Magn. Reson. Spectrosc.*, 1999, **3**, 203; (c) Y. Cohen, L. Avram and L. Frish, *Angew. Chem. Int. Ed.*, 2005, **44**, 520.
9. (a) R. Dobrawa, M. Lysetska, P. Ballester, M. Grüne and F. Würthner, *Macromolecules*, 2005, **38**, 1315; (b) F. Würthner, V. Stepanenko and A. Sautter, *Angew. Chem. Int. Ed.*, 2006, **45**, 1939.